Interaction of Poly(amidoamine) Dendrimers with Supported Lipid Bilayers and Cells: Hole Formation and the Relation to Transport

Seungpyo Hong,[§,▽] Anna U. Bielinska,[‖,▽] Almut Mecke,[⊥,▽] Balazs Keszler,[‖,▽] James L. Beals,[‖,▽] Xiangyang Shi,[‖,▽] Lajos Balogh,[§,‖,▽] Bradford G. Orr,[†,⊥,▽] James R. Baker, Jr.,[‖,▽] and Mark M. Banaszak Holl*,[†,‡,§,⊗,▽]

Programs in Applied Physics, Biophysics, and Macromolecular Science and Engineering, Departments of Internal Medicine, Physics, and Chemistry, and Center for Biologic Nanotechnology, University of Michigan, Ann Arbor, Michigan 48109. Received February 17, 2004; Revised Manuscript Received May 4, 2004

We have investigated poly(amidoamine) (PAMAM) dendrimer interactions with supported 1,2-dimyristoyl-sn-glycero-3-phosphocholine (DMPC) lipid bilayers and KB and Rat2 cell membranes using atomic force microscopy (AFM), enzyme assays, flow cell cytometry, and fluorescence microscopy. Amine-terminated generation 7 (G7) PAMAM dendrimers (10−100 nM) were observed to form holes of 15−40 nm in diameter in aqueous, supported lipid bilayers. G5 amine-terminated dendrimers did not initiate hole formation but expanded holes at existing defects. Acetamide-terminated G5 PAMAM dendrimers did not cause hole formation in this concentration range. The interactions between PAMAM dendrimers and cell membranes were studied in vitro using KB and Rat 2 cell lines. Neither G5 amine- nor acetamide-terminated PAMAM dendrimers were cytotoxic up to a 500 nM concentration. However, the dose dependent release of the cytoplasmic proteins lactate dehydrogenase (LDH) and luciferase (Luc) indicated that the presence of the amine-terminated G5 PAMAM dendrimer decreased the integrity of the cell membrane. In contrast, the presence of acetamide-terminated G5 PAMAM dendrimer had little effect on membrane integrity up to a 500 nM concentration. The induction of permeability caused by the amine-terminated dendrimers was not permanent, and leaking of cytosolic enzymes returned to normal levels upon removal of the dendrimers. The mechanism of how PAMAM dendrimers altered cells was investigated using fluorescence microscopy, LDH and Luc assays, and flow cytometry. This study revealed that (1) a hole formation mechanism is consistent with the observations of dendrimer internalization, (2) cytosolic proteins can diffuse out of the cell via these holes, and (3) dye molecules can be detected diffusing into the cell or out of the cell through the same membrane holes. Diffusion of dendrimers through holes is sufficient to explain the uptake of G5 amine-terminated PAMAM dendrimers into cells and is consistent with the lack of uptake of G5 acetamide-terminated PAMAM dendrimers.

INTRODUCTION

Poly(amidoamine) (PAMAM) dendrimers have demonstrated great promise for a variety of biomedical applications. This class of polymers has a number of favorable properties including well-defined chemical structure, globular shape, low polydispersity index (close to 1.0), biocompatibility, and controlled terminal functional groups. Amine-terminated PAMAM dendrimers have proven to be effective as a nonviral cell transfection agent (*1*, *2*). Modification of the PAMAM dendrimer surface functional groups with targeting compounds, fluorescent groups, and drugs have produced promising imaging and therapeutic agents (*3*−*7*).

The success of PAMAM dendrimers in biomedical applications such as those mentioned above raises the question regarding how PAMAM dendrimers interact with cell membranes at the molecular level. The complex structure of cell membranes has prompted several research groups to employ phosphatidylethanolamine-containing vesicles as model systems. Efficient cross-membrane transport and membrane disruption were observed with a strong dependence on dendrimer size (generation), chemical structure of the dendrimer, and composition of the model membranes (*8*−*10*). Based upon these studies, the internalization mechanism of dendrimers into cells has been explained as a dendrimer-mediated endocytosis. Endocytosis is a complex multistep process and can be generally described in terms of cell transfection efficiency. A cationic polymer (e.g. poly-(lysine) or PAMAM dendrimer) is proposed to bind with the outer cell membrane and be internalized into the cell through endocytosis. The polymer then exits from the endosome, which is a step that controls the transfection efficiency (*11*). The electrostatic interaction between the polymer and the lipid bilayer membrane and concomitant osmotic imbalance have been understood as important driving forces for polycation-mediated endocytosis (*10*, *12*). Other oligomers that may follow similar pathways include the cell-penetrating peptides (CPPs) such as Tat and oligoarginine (*13*, *14*).

The model systems studied to date show good evidence for membrane disruption by PAMAM dendrimers (*8*, *10*).

* To whom correspondence should be addressed. Phone: (734) 763-2283. Fax: (734) 763−2307. E-mail: mbanasza@umich.edu.
† Program in Applied Physics.
‡ Program in Biophysics.
§ Program in Macromolecular Science and Engineering.
‖ Department of Internal Medicine.
⊥ Department of Physics.
⊗ Department of Chemistry.
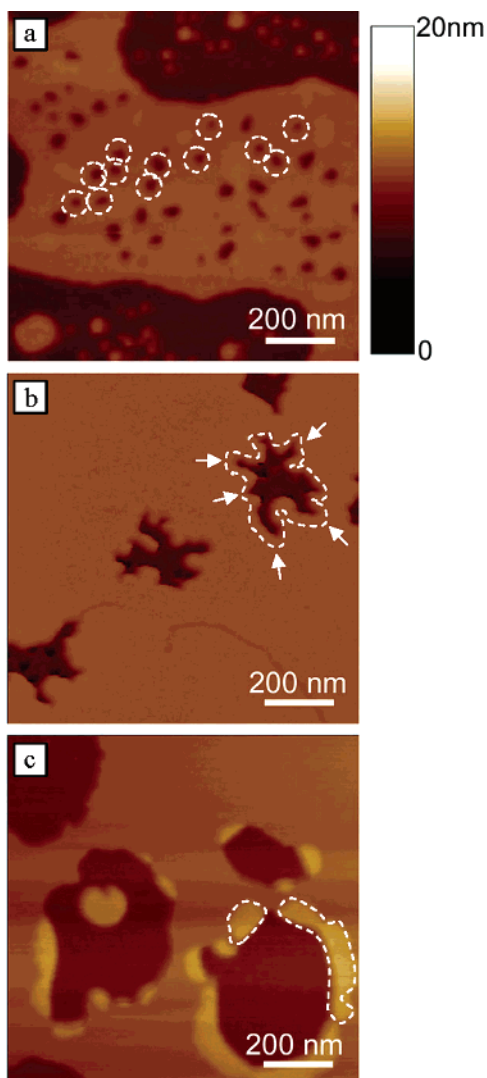▽ Center for Biologic Nanotechnology.

Figure 1. AFM height images of DMPC bilayer after interaction with dendrimers. White lines highlight some of the areas where dendrimers have affected the bilayer (the dendrimer themselves cannot be seen on these images). (a) G7-NH$_2$ cause the formation of small holes, 15−40 nm in diameter, in the previously intact parts of the bilayer (see dark spots). (b) G5-NH$_2$ remove lipid molecules primarily from edges of existing bilayer defects, i.e., dark areas grow in size, see arrows. (c) G5-Ac do not remove lipid molecules from the surface. Instead they adsorb to edges of existing bilayer defects.

However, they do not provide direct evidence for the nature of the membrane/dendrimer interaction or the endocytosis process. To study this interaction in greater detail, we have used atomic force microscopy (AFM) to directly image supported DMPC lipid bilayers upon exposure to PAMAM dendrimers. The results of this study are summarized in Figure 1 (*15, 16*). G7 with amine-terminated surfaces (G7-NH$_2$) generated 15−40 nm-size holes in the bilayer (Figure 1a). In the case of G5-NH$_2$, however, few new holes were observed (Figure 1b). Instead, the dendrimer removed lipid molecules from edges of existing bilayer defects expanding the size. Amine-terminated dendrimers are protonated in neutral water (*9, 17*) and therefore can be anticipated to have a substantial electrostatic interaction with the DMPC lipid. The G7-NH$_2$ has a larger number of primary amine groups (512) than the G5-NH$_2$ (128) at the same molar concentrations, resulting in a greater charge density. G7-NH$_2$ also has a larger radius of curvature. These two

physical differences likely contribute to the higher level of membrane disruption for the G7 dendrimer. Varying the chemical functionality of the surface significantly changed the outcome of the interaction. Acetamide-terminated G5 PAMAM dendrimer (G5-Ac) did not result in hole formation or the expansion of existing defects. Instead, G5-Ac intercalated at edges of preexisting bilayer defects (Figure 1c). These results illustrate that holes are formed and/or expanded in DMPC-supported bilayers by the addition of G7-NH$_2$ or G5-NH$_2$ (both positively charged in neutral water). The addition of neutral G5-Ac dendrimer does not cause hole formation at 10−100 nM concentrations. This set of results is particularly striking because PAMAM dendrimers must have charge-neutralized surfaces for selective drug delivery applications (*3, 18*). These results confirm that amine-terminated materials show undesirable nonselective uptake into tested cell types. In contrast, the amine-terminated dendrimers are highly efficient nonspecific transfection agents while the acetamide-terminated polymers do not transfect cells.

The AFM experiments on supported lipid bilayers suggest the following hypotheses: (1) amine-terminated PAMAM dendrimers can induce the formation of holes in cell membranes, (2) the holes generated in the cell membranes allow the diffusion of molecules into and out of the cell, (3) acetamide-terminated dendrimers do not enter cells because they do not interact with membrane phospholipids and generate holes.

In this paper, we test the three hypotheses by investigating the interaction of G7-NH$_2$, G5-NH$_2$, and G5-Ac PAMAM dendrimers with KB and Rat2 cell membranes. We have evaluated the release of two cytosolic enzymes, lactate dehydrogenase (LDH) and luciferase (Luc), from the cells upon exposure to dendrimers in terms of generation and the identity of surface functional group (amine or acetamide). The temperature dependence of the binding and internalization has also been studied. It was found that G7-NH$_2$ and G5-NH$_2$ PAMAM dendrimers induce significant leakage of LDH and Luc whereas G5-Ac does not. Similarly, the presence of G5-NH$_2$ was shown to make the cell membrane permeable to the small molecules such as propidium iodide (indicating diffusion into cells) and fluorescein (indicating diffusion out of cells) even though the cell was still viable. These results, in addition to others discussed in this paper and the AFM data illustrated in Figure 1, provide direct experimental support for hypotheses 1, 2, and 3.

EXPERIMENTAL PROCEDURES

Preparation of Materials. Generation 5 and 7 PAMAM dendrimers were synthesized at the Center for Biologic Nanotechnology, University of Michigan. All other chemicals were acquired from Aldrich and used without further purification. Water used in this work was purified by Milli-Q Plus 185 system and had a resistivity higher than 18 MΩ/cm. The PAMAM dendrimers were purified using ultrafiltration and dialysis (*2*). Purified PAMAM dendrimers were then acetamide capped using triethylamine (20% mol excess to acetic anhydride) as a proton acceptor as described in the literature (*18*). Folic acid (FA) was conjugated to G5 PAMAM dendrimers after partial acetylation, followed by full acetylation (*3*). Numbers of primary amine end groups were measured by potentiometric titration (*18*) and numbers of modified end groups were calculated based upon the titration result of the starting G5-NH$_2$.

Scheme 1. End Group Modification of PAMAM Dendrimers Investigated in This Study: Amine End Groups (−NH₂, Generations 5 and 7) and Acetamide End Groups (−NHCOCH₃, Generation 5)[a]
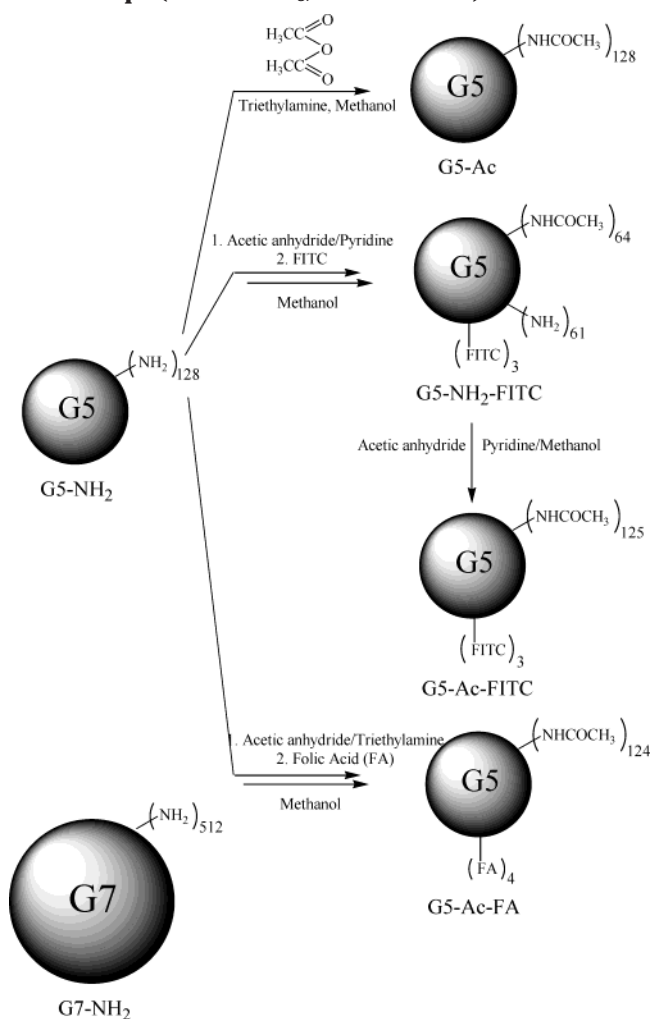
[a] Note that the numbers of end groups and functional groups are given as the theoretical values in this scheme.

Dendrimer−fluorescein conjugates were obtained as follows. G5-NH₂ (54.4 mg) in 5 mL of methanol was acetylated by adding 11.7 mg of acetic anhydride in an equal volume of methanol and vigorously stirring the mixture for 24 h, resulting in acetylation of half the primary amine groups (Scheme 1). Fluorescein isothiocyanate (FITC) (2.62 mg) in 10 mL of methanol was then added, and the mixture was stirred for 24 h. 10 mL of the reaction mixture was then dialyzed against 0.5 M NaCl solution followed by dialysis against water (six times, 4 L) for 3 days to remove methanol solvent and unreacted small molecules. The water was removed using a rotary evaporator, and the resulting solids were redissolved into 3−5 mL of water. Lyophilization for 3 days produced solid G5-NH₂−FITC conjugate. The remaining 10 mL of the reaction mixture including unpurified G5-NH₂−FITC conjugate and unreacted small molecules was fully acetylated and purified, resulting in G5-Ac−FITC.

Identification of Dendrimer Conjugates. The dendrimer-based conjugates (G5-Ac−FA, G5-NH₂−FITC, and G5-Ac−FITC) were analyzed by UV/vis spectroscopy. The maximum absorbance (λ_{max}) of FA was shifted from 280 to 289 nm after conjugation, indicating that FA was conjugated to the PAMAM. Absorbance peaks of free FITC appeared at wavelengths of 270 and 490 nm. After

the conjugation reaction, the FITC peaks were shifted to 280 and 500 nm, respectively. Further purification of synthesized dendrimers was performed by repeated ultrafiltration, dialysis with water and methanol, and lyophilization (*3, 19*). The dendrimer−FITC conjugates were also evaluated by gel eletrophoresis after purification using agarose gel with 2% ethidium bromide to confirm that the polymers have the desired charged groups and no impurities are present such as free FITC.

MALDI-TOF measurements were carried out using a Waters Tofspec-2E (Milford, MA) using the linear delayed extraction mode. The instrument was calibrated with a mixture of known proteins in a sinapinic acid matrix before use. Five microliters of each sample solution in ultrapure water/methanol (50/50 by vol %) was mixed with 5 μL of matrix solution, and 1 μL spots were placed on the target. The matrix solution was 2,5-dihydroxy-benzoic acid (Aldrich, Milwaukee, WI), dissolved in 50/50 acetonitrile/water with 0.1% TFA, at a concentration of 10 mg/mL. Five laser shots were added per spectrum, and multiple spectra were added together. The mean smoothing algorithm was applied to the data, and the baseline was subtracted. A comparison between theoretical and experimental molar masses is provided in Table 1.

Preparation and AFM Measurement of Supported DMPC Lipid Bilayers. DMPC lipid bilayers were chosen since these phospholipids are an important part of mammalian cell membranes, and the lipid bilayers are easily accessible to high-resolution imaging by AFM under physiological conditions. DMPC was purchased from Avanti Lipids, Alabaster, AL. A 0.5−0.7 mg/mL suspension of small, unilamellar vesicles (SUVs) was prepared using literature procedures (*15*). Supported lipid bilayers were formed by depositing 80 μL of liposome suspension on a piece of freshly cleaved mica. After an incubation time of about 20 min, the sample was gently rinsed with water to remove excess lipids and placed in the AFM for imaging as described elsewhere (*15*). All AFM measurements were performed in tapping mode on a Nanoscope IIIa Multimode scanning probe microscope from Digital Instruments (DI, Veeco Metrology Group, Santa Barbara, CA). The AFM was equipped with a liquid cell (DI) and a silicone nitride cantilever (DI model NPS, spring constant 0.32 N/m, length 100 μm) operating at a drive frequency of about 6−9 kHz. After taking an initial image of the bilayer, 20−30 μL of dilute dendrimer solution was injected into the liquid cell. The resulting dendrimer concentrations were in the range of 10−100 nM. After adding the dendrimers, imaging continued to observe their effect on the bilayer.

Cell Lines. The KB and Rat2 cell lines were purchased from the American Type Tissue Collection (ATCC; Manassas, VA) and grown continuously as a monolayer at 37 °C, and 5% CO₂ in RPMI 1640 medium (Mediatech, Herndon, VA) and Dulbecco's modified Eagle's medium (DMEM, Gibco, Eggenstein, Germany), respectively. Both cell lines were transfected to permanently express the Luc gene using PAMAM dendrimer-mediated gene transfection as previously reported (*1, 20*). The Luc expressing KB and Rat2 Cells are noted as KBpLuc and Rat2pLuc, respectively. The RPMI 1640 and DMEM media were supplemented with penicillin (100 units/mL), streptomycin (100 μg/mL), and 10% heat-inactivated fetal bovine calf serum (FBS) before use. Folic acid receptor expressing KB cell line (FAR-KB) was also used for specific binding with G5-Ac−FA. The KB cell line for specific binding was cultured in the RPMI 1640 medium without

Table 1. Molar Mass and Chemical Composition of the Dendrimers Employed in This Study

dendrimers	no. of amine terminal groups	no. of acetamide terminal groups	no. of FITC	no. of FA	theoretical molar mass[d]	experimental molar mass[e]
G5-NH₂	110[a]	-	-	-	28826	28260
G5-Ac	0	110[b]	-	-	32880	32254
G5-NH₂−FITC	51[c]	55[c]	3[c]	-	29939	29820
G5-Ac−FITC	0	106[c]	3[c]	-	32081	31186
G5-Ac−FA	13[c]	93[c]	-	4[c]	33394	32519

[a] Measured by potentiometric titration. [b] Calculated from titration result of G5-NH₂. [c] Determined by stoichiometry of the conjugation reaction based on the titration data of starting G5-NH₂. [d] Theoretical molar mass values for G5-Ac, G5-NH₂−FITC, G5-Ac−FITC, and G5-Ac−FA are calculated based upon the experimental molar mass of the G5-NH₂ starting material employed. Note that G5-Ac and G5-Ac−FA were prepared from G5-NH₂ containing 110 primary amine groups and having a molar mass of 28,260 as measured by MALDI-TOF. The G5-NH₂−FITC and G5-Ac−FITC were prepared from starting G5-NH₂ with 109 primary amine groups and molar mass of 26,462 as measured by MALDI-TOF. [e] Measured by MALDI-TOF spectroscopy.

folic acid (Mediatech, Herndon, VA) for at least 4 days, resulting in the FAR-KB cell line.

Luc and LDH Assays. To assess the release of cytosolic enzymes caused by general toxicity, the cytotoxicity of the G5 dendrimers was preassayed using a BCA protein assay (*21*). The assay results show that the both G5-NH₂ and G5-Ac are not cytotoxic up to a 500 nM concentration (>90% cell viability). Based on this information, the assays performed to investigate the cytosolic enzyme release were carried out in a dendrimer concentration range of 10−500 nM. Within this range, dendrimers are non-cytotoxic so the observed enzyme release can be ascribed to an increase in cell membrane permeability as opposed to general lysis due to cell death.

A concentration of 5×10^4 cells/well of both KBpLuc and Rat2pLuc cells were seeded on 24-well plates to prepare cell monolayers. After 24 h, cell culture media were removed and replaced by 300 μL/well of dendrimer/PBS (Ca²⁺, Mg²⁺) solutions at various dendrimer concentrations. Cells were incubated either at 6 or 37 °C at 5% CO₂. The supernatants were then collected at specific time points ranging from 1 h to 3 h. Cell debris were removed by centrifugation of the supernatant (at 400 × g for 2 min).

The LDH activity in the cell supernatant was analyzed using an LDH assay kit (Promega Co., Madison, WI). The supernatant (20 μL) was mixed with 50 μL of reagent solution, incubated at room temperature for 30 min, followed by adding 50 μL of stop solution (acetic acid). The change in absorbance (proportional to LDH activity) was measured at 490 nm at room temperature using Spectra Max 340 ELISA Reader (Molecular Devices, Sunnyvale, CA) spectrophotometer. Luc activity was quantified using a chemiluminescence assay. Light emission from collected supernatants (10 μL) incubated with 2.35×10^{-2} μmol of luciferin substrate (Promega Co., Madison, WI) was measured in the chemiluminometer (LB96P; EG & G/Berthold, Gaithersburg, MD). The measured LDH and Luc activities were either adjusted for the protein concentration of the sample or recalculated by percentage to the activities of cell lysates of intact cells.

Fluorescence Microscopy Observation. Rat2 cells (4×10^4) were seeded on six MatTek glass-bottom Petri dishes (35 mm) and incubated at 37 °C under 5% CO₂ for 24 h. The media was removed, and 2 mL of dendrimer−FITC conjugate/PBS (Ca²⁺, Mg²⁺) solution was added. Three dishes were incubated with added dendrimer solutions at 37 °C under 5% CO₂ for 1 h. The other three dishes were precooled at 6 °C for 30 min before adding the dendrimer solutions and incubated with the dendrimer solution at 6 °C for 1 h. Dendrimer solutions were removed, and the resulting cell monolayer was washed with PBS. Cells were fixed with 2% formaldehyde
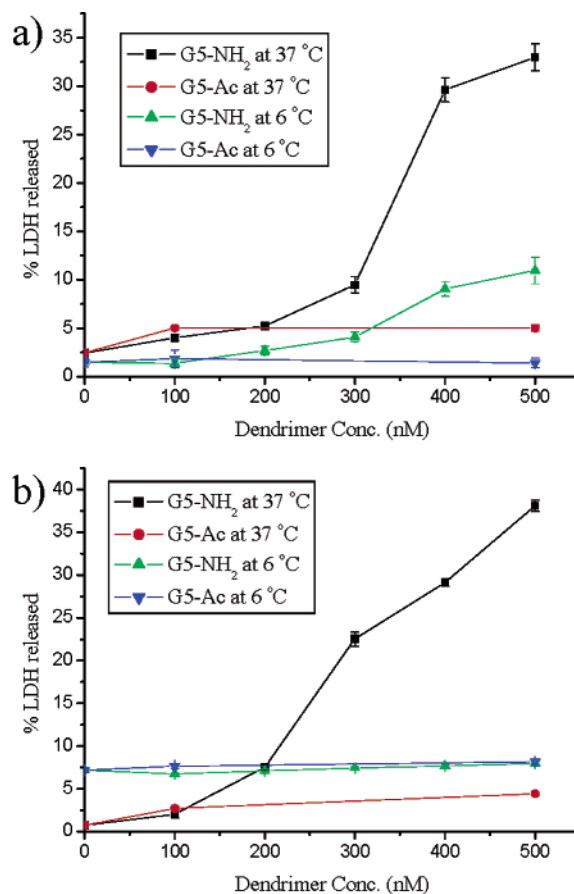

Figure 2. Dose-dependent LDH release from (a) KBpLuc and (b) Rat2pLuc cell lines at 37 °C and 6 °C by G5-NH₂ and G5-Ac PAMAM dendrimers.

in the PBS (Ca²⁺, Mg²⁺) at room temperature for 10 min, followed by washing with PBS twice. DNA in the cell nucleus was then stained by DAPI. The samples were imaged with a Nikon diaphot 200 inverted microscope, using appropriated filters and dichroic to image FITC (465−495 nm excitation, 505 nm dichroic, 515−555 nm emission). A mercury vapor lamp was the light source for the epiflourescense imaging. Nikon 20× plan Apo 0.9 na was used as an objective. Images were captured with an Orca-ER16 bit gray scale CCD. The light path filters were controlled with Sutter Instrument Company's Lambda N2 TTL controller, and the camera was driven with Compix software.

Assessment of Reversibility of Dendrimer-Induced Membrane Permeability. Four wells with 5×10^4 Rat2 cells were prepared for each particular dendrimer concentration resulting in 16 wells in total. The supernatants were removed from two wells out of four
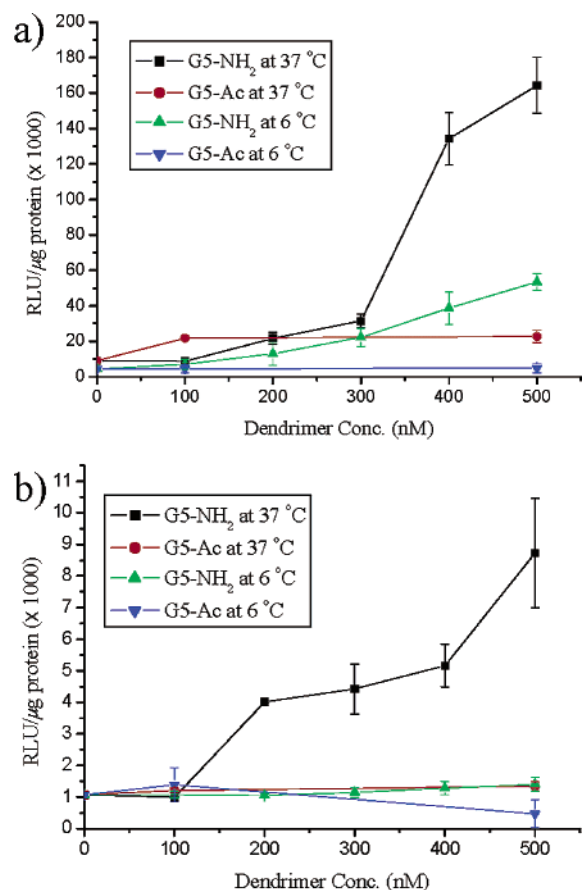
Figure 3. Dose-dependent Luc release from (a) KBpLuc and (b) Rat2pLuc cell lines at 37 °C and 6 °C by G5-NH$_2$ and G5-Ac PAMAM dendrimers.

wells after 1 h incubation and assayed using the techniques described above for LDH. These wells were then replaced with PBS and assayed again after an additional2 h. The other two wells were incubated with G5-NH$_2$ dendrimer solutions for 3 h and also assayed.

PI and FDA Staining and Flow Cytometry. The cells were stained with propidium iodide (PI; Molecular Probes, Eugene, OR) and fluorescein diacetate (FDA; Molecular Probes, Eugene, OR) by modification of a protocol described previously (*22*). One milliliter of 2.5 × 10^5 KB and Rat2 cells was seeded in 12-well plates and incubated at 37 °C under 5% CO$_2$ for 24 h. FDA staining was performed as follows. The media was removed, and 50 μL of 10 mg/mL FDA/H$_2$O solution was added. Dendrimer/PBS solution (300 μL) was then added after 30 min and incubated for another 30 min. For PI staining, 300 μL of dendrimer/PBS solution was added after removal of cell culture media followed by addition of 50 μL of 10 mg/mL PI/H$_2$O solution. For both PI and FDA staining, total incubation time was 1 h. After the incubation, cells were trypsinized with trypsin−EDTA and centrifuged at 1200 rpm for 5 min. Resulting cell pellets were then resuspended in PBS with 0.1% bovine serum albumin (BSA).

The fluorescence signal of individual cells was assessed with a Coulter EPICS/XL MCL Beckman-Coulter flow cytometer and data were analyzed using Expo32 software (Beckman-Coulter, Miami, FL) (*23, 24*).

RESULTS

Dendrimer-Induced Enzyme Leakage from Cells. The effects of G7-NH$_2$, G5-NH$_2$, and G5-Ac dendrimers
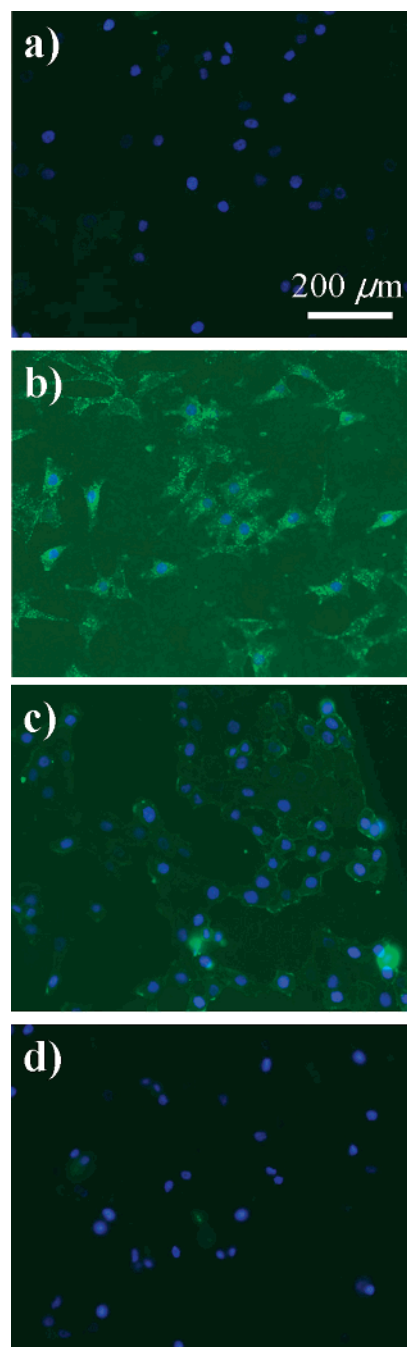

Figure 4. Fluorescence microscopy of (a) untreated Rat2 cells (control), (b) Rat2 cells incubated with 200 nM G5-NH$_2$−FITC at 37 °C for 1 h, (c) Rat2 cells incubated with 200 nM G5-NH$_2$−FITC at 6 °C for 1 h, and (d) Rat2 cells incubated with 200 nM G5-Ac−FITC at 37 °C for 1 h. Blue spots represent the cell nucleus stained by DAPI and green spots are dendrimer−FITC conjugates.

on the membrane permeability of KB and Rat2 cells were investigated using LDH and Luc assays. Concentration dependent dendrimer-induced LDH release at 37 and 6 °C is shown in Figure 2. As the concentration of G5-NH$_2$ increases, the LDH release from both KBpLuc and Rat2pLuc increases. In contrast, neither cell line releases a significant amount of LDH as a result of exposure to G5-Ac. KBpLuc and Rat2pLuc cells incubated with both G5-NH$_2$ and G5-Ac at 6 °C exhibited no LDH release. Luc release followed the same general trend observed for LDH release (Figure 3).

Binding and Internalizaton of Dendrimers. To investigate the binding and internalization of den-
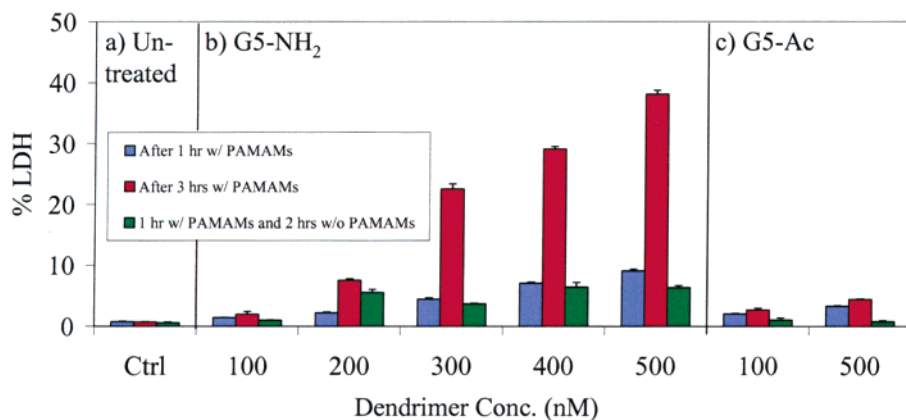
Figure 5. Enzyme release of Rat2 incubated with (a) G5-NH$_2$ and (b) G5-Ac. Light blue and red bars represent the release after 1 h and 3 h incubation with dendrimer solutions, respectively. Green bars represent enzyme release after 1 h incubation with dendrimers followed by washing and 2 h incubation in pure PBS buffer to allow recovery of membrane integrity.
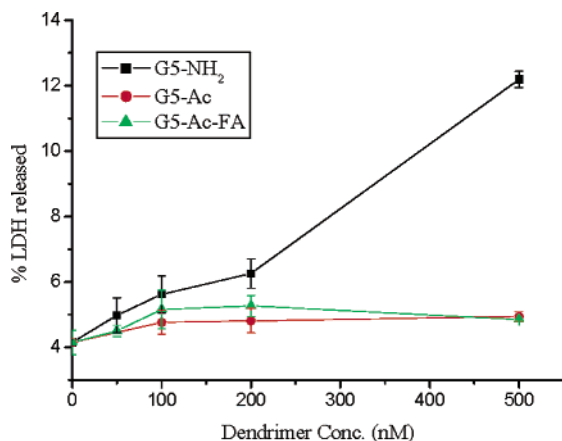

Figure 6. Comparison of interaction of G5-NH$_2$, G5-Ac, and G5-Ac−FA with FAR-KB cell line. Note that G5-Ac−FA is internalized by receptor-mediated endocytosis.

drimers, fluorescence images of Rat2 cells were taken after incubation with dendrimer−FITC conjugates at different temperatures. Rat2, a fibroblast cell line, was chosen in this experiment due to its stable surface adherence. DNA in the cell nucleus was stained by DAPI. The stained nuclei can be seen as blue spots in Figure 4a−d while dendrimer−FITC conjugates emit green fluorescence. Figure 4b shows a fluorescence image of Rat2 cells incubated with 200 nM of G5-NH$_2$−FITC at 37 °C for 1 h. Dendrimers are apparent both inside the cells as well as associated with the membrane. This indicates that the G5-NH$_2$−FITC dendrimers interact with the cell membrane and enter the cell at physiological temperature (37 °C). At 6 °C, however, although the dendrimers associate with the cell membrane, no signifi-cant internalization was observed (Figure 4c). Identical experiments employing G5-Ac−FITC at 200 nM concen-tration indicate no association with the cell membrane nor internalization into the cell (Figure 4d).

Reversibility of Dendrimer-Induced Membrane Permeability. Testing the reversibility of the den-drimer-induced membrane permeability was performed by replacing a solution of G5-NH$_2$ dendrimer with a dendrimer-free PBS and monitoring the LDH release. The dendrimer-induced membrane permeability of cell lines in the presence of G5-NH$_2$ was not permanent and cells recovered their membrane integrity upon removal of dendrimer/PBS solutions (Figure 5), as indicated by LDH release. This "resealing" behavior is consistent with the observation that G5-NH$_2$ dendrimers are not cytotoxic
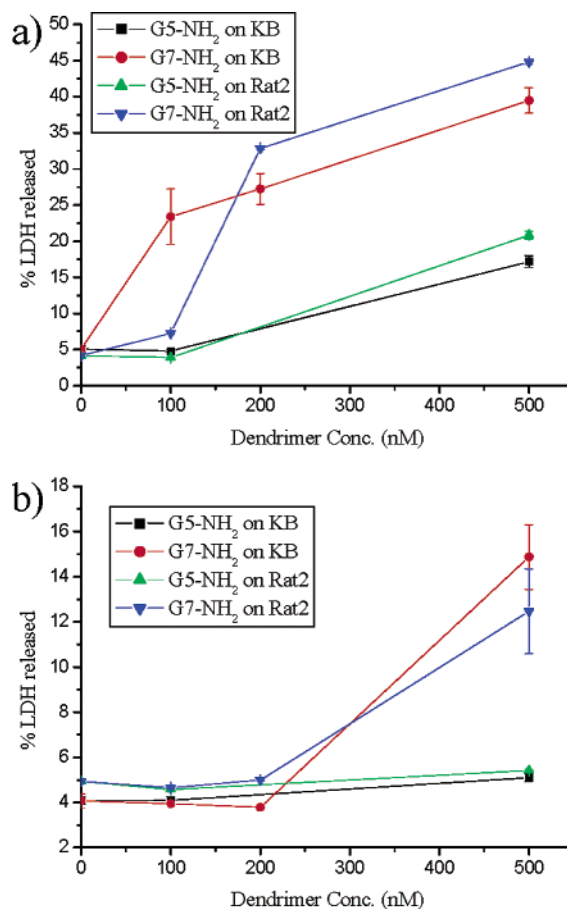

Figure 7. Comparison of different dendrimer generations: Enzyme release from KB and Rat2 cells after incubation with G5-NH$_2$ and G7-NH$_2$ at (a) 37 °C and (b) 6 °C.

up to 500 nM as after removal of the dendrimer solution. The cell can return the membrane permeability back to the normal level.

The Role of Dendrimer Surface Functionaliza-tion: Amine vs Acetamide. To test possible mecha-nisms of internalization and their implications for cyto-solic enzyme release (Figure 6), comparisons between G5-NH$_2$, G5-Ac, and G5-Ac−FA were carried out using the LDH assay. It has been demonstrated that internaliza-tion of G5-Ac−FA occurs through receptor-mediated endocytosis, initiated by binding of folic acid (FA) to folic acid receptors (FAR) on KB cells (*3*). Under the same conditions, no uptake of G5-Ac is observed. The LDH

assay results show no significant LDH release from KB cells following a 3-h incubation with G5-Ac–FA or G5-Ac. However, incubation with G5-NH$_2$ induced significant LDH release, consistent with previous experiments.

Effect of Dendrimer Generation on Cell Membrane Permeability. It is well-known that high generation PAMAM dendrimers are unusually effective at disrupting cell membranes (*10*, *25*). We also observed a distinct difference in the ability to form holes in supported DMPC bilayers (Figure 1). To test this effect upon LDH release, G5-NH$_2$ and G7-NH$_2$ dendrimers were analyzed at 37 and 6 °C. The results of an LDH assay comparing enzymatic leakage for both KB and Rat2 cell lines after exposure to varying concentration of G5-NH$_2$ and G7-NH$_2$ are shown in Figure 7. At 37 °C, G7-NH$_2$ causes a greater release of LDH than G5- NH$_2$ at all concentrations. In addition, whereas LDH release was not observed for G5-NH$_2$ at 6 °C, the G7-NH$_2$ was still capable of causing LDH release (Figure 7b).

Are Holes Present in the Cellular Membrane? Tests for Diffusion of Dyes. To study passive diffusion in and out of the cell, small molecular probes (PI and FDA) were used according to a modification of a previous literature method (*22*). PI is readily internalized into cells with disrupted membranes but is excluded from cells with intact membranes. On the other hand, FDA, a nonfluorescent compound, readily enters intact cells and then undergoes hydrolysis by endogenous esterase, resulting in release of fluorescein into the cytosol. The cytosolic fluorescein is not able to transverse a normal cell membrane without holes. Thus, the FDA is used as a marker for diffusion-out. Consequently, it is presumed that fluorescence intensity of PI should be increased and that of fluorescein should be decreased if the presence of G5-NH$_2$ makes the membrane permeable to these dyes.

Figure 8 shows flow cytometer data of Rat2 cells incubated with G5 PAMAM dendrimers and then stained with PI. As illustrated in Figure 8a–c and 8e, PI is internalized into the cells in a G5-NH$_2$ concentration dependent manner. In the case of G5-Ac, however, no significant difference in PI incorporation was observed as compared to the control cells (Figure 8d,e).

Fluorescence intensity of fluorescein in cells as a function of G5-NH$_2$ dendrimer concentration is illustrated in Figure 9. Consistent with previous results (*22*), FDA was internalized through intact cell membranes, resulting in a substantial signal for free fluorescein in Rat2 cells. As the G5-NH$_2$ concentration increased, however, the signal intensity of the fluorescein significantly decreased, indicating that the membrane had become permeable (Figure 9e). Rat2 cells incubated with G5-Ac did not show any noticeable difference from the control experiment (Figure 9d).

DISCUSSION

Summary of Evidence for PAMAM-Induced Hole Formation in the Cell Lipid Bilayer. AFM observation (Figure 1) of holes formed in DMPC lipid bilayers triggered our in vitro experiments to investigate the interactions between dendrimers and viable cell membranes. The release of cytosolic enzymes, LDH and Luc, demonstrates an increase in membrane permeability (Figures 2 and 3). The increased permeability is consistent with the hypothesis of PAMAM-induced hole formation in the cell lipid bilayer. The larger enzyme of the two, LDH, is a 135–140 kDa complex protein with a hydrodynamic radius of ~4.3 nm (*26*). Thus, it is small enough to fit through the 15–40 nm holes suggested by
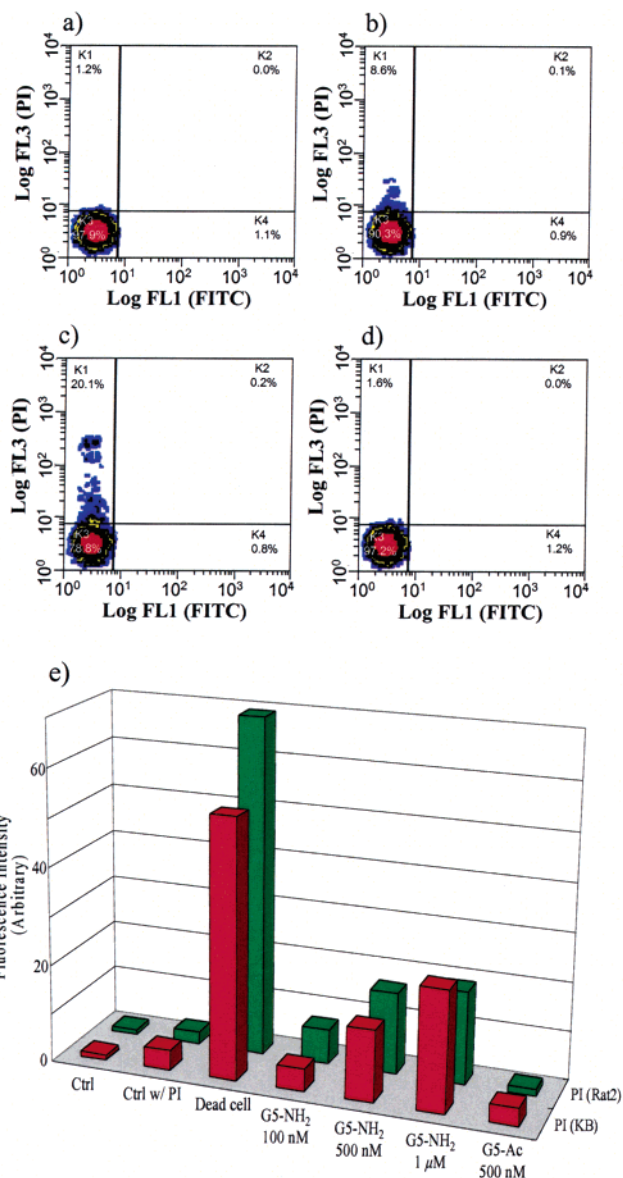

Figure 8. Flow cytometer diagrams of Rat2 cells at several representative conditions. (a) untreated, (b) incubated with PI, (c) incubated with 500 nM G5-NH$_2$ and PI, and (d) incubated with 500 nM G5-Ac and PI at 37 °C for 1 h. (e) Signal intensity of PI fluorescence for KB and Rat2 cells after incubation with dendrimers. Controls (first three columns): cells in pure PBS buffer, cells in the buffer with PI, and dead cells incubated with 30% ethanol solution for 30 min.

the AFM experiment. The smaller 62 kDa enzyme, Luc composed of α- and β-subunits, should be able to diffuse through the hole. The overall dimensions of this heterodimer are reported as 7.5 nm × 4.5 nm × 4.0 nm (~2.7 nm in radius) (*27*). Membrane permeability returns to normal following removal of the dendrimer-containing solution. In contrast to the supported lipid bilayer, where holes remain for a relatively long time, the cell has additional lipid available and the membrane can regenerate its membrane within 2 h (as assayed by permeability in Figure 5).

Although permeability to cytosolic enzymes is consistent with hole formation, the possibility that cytosolic enzymes leak out during an endocytosis process must be addressed. This is a particularly important issue since amine-terminated PAMAM dendrimers, protonated in aqueous solution, have been proposed to enter cells via an endocytosis mechanism (*11*). However, experiments
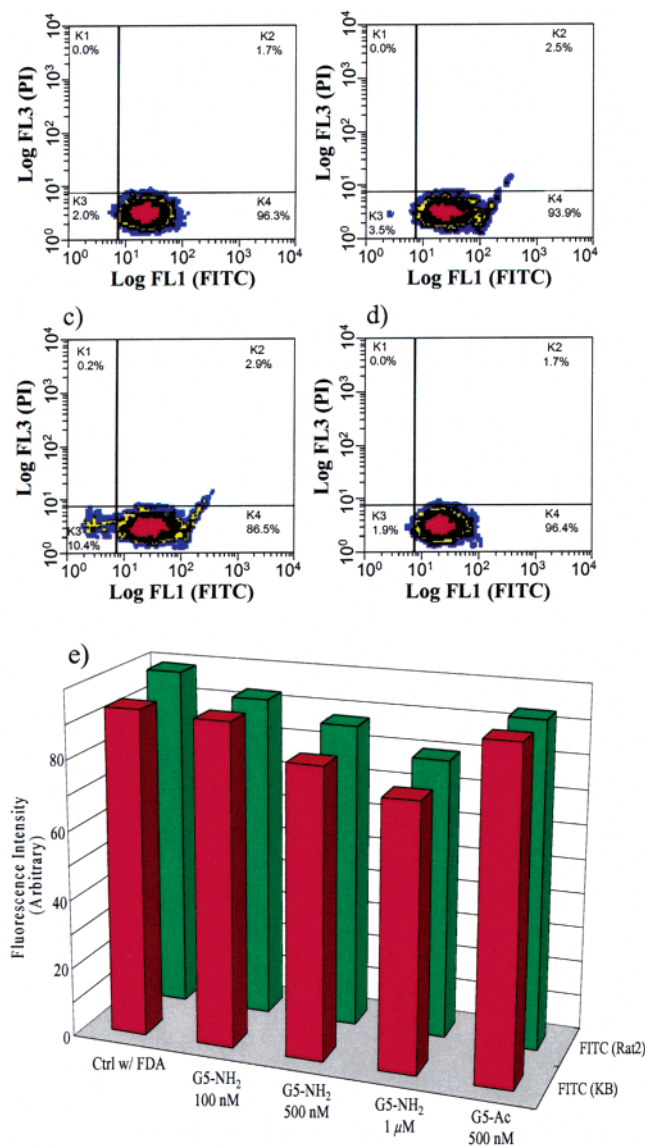
Figure 9. Flow cytometer diagrams of Rat2 cells at several representative conditions. (a) untreated, (b) incubated with FDA and 500 nM G5-NH$_2$, (c) incubated with FDA and 1 μM G5-NH$_2$, and (d) incubated with FDA and 500 nM G5-Ac at 37 °C for 1 h. (e) Signal intensity of fluorescein fluorescence for KB and Rat2 cells after incubation with dendrimers. Control (first column): cells with FDA in PBS buffer.

using G5-Ac−FA, a material known to undergo endocytosis via the folic acid receptor, did not cause leakage of LDH or Luc (Figure 6). This demonstrates that noncharged PAMAM dendrimers can enter the cell via receptor-mediated endocytosis without causing cytosolic enzyme leakage (*13*, *14*). However, we still cannot rule out the possibility that the G5-NH$_2$ dendrimer undergoes an endocytosis process sufficiently different in mechanism to cause leakage. To test this possibility, we examined the behavior of two common dyes in the presence of G5-NH$_2$ and G5-Ac dendrimers.

PI and FDA were used respectively as tests for the mechanistic process of diffusion in and out of the cells. If dendrimer-induced holes are present, the dyes would be expected to diffuse in and out of the cell, respectively. However, the positively charged PI would be repelled from the polycationic G5-NH$_2$ dendrimer in aqueous solution and would not be anticipated to accompany the dendrimer during endocytosis. The experimental data shows that as G5-NH$_2$ concentration increases, PI signal

intensity is increased while FITC intensity is decreased (Figures 8 and 9). The diffusion behavior of these small molecular probes is consistent with the formation of small holes in the membrane. The PI data is inconsistent with the molecules accompanying a polycation-mediated endocytosis.

To further test the possibility of an endocytosis mechanism, we examined the temperature dependence of cytosolic enzyme leakage (Figures 2, 3, 4, and 7). At 6 °C, no enzyme leakage is observed for G5-NH$_2$ dendrimers at concentrations showing substantial leakage at 37 °C. This is consistent with either endocytosis or hole formation mechanisms as both would be expected to be temperature dependent. When G7-NH$_2$ dendrimer is employed at 6 °C, however, cytosolic enzyme leakage can again be observed. Note that endocytosis processes will be just as disfavored as for the G5-NH$_2$ case. However, as indicated in Figure 1, G7-NH$_2$ has a greater propensity to form holes. Thus, it is not surprising that G7-NH$_2$ can continue to cause hole formation in the cell plasma membrane.

Taken as a whole, the leakage of the cytosolic enzymes, the free diffusion of PI and FITC dye, and the direct observations made by fluorescence microscopy as shown in Figures 2, 3, 4, 7, 8, and 9 provide experimental support for hypotheses 1 and 2: (1) amine-terminated PAMAM dendrimers can induce the formation of holes in cell membranes, and (2) the holes generated in the cell membranes allow the diffusion of polymers, enzymes, and molecules into and out of the cell. In addition, these data support hypothesis 3 that acetamide terminated dendrimers do not cause holes (Figure 1) or induce enzyme release (Figures 2 and 3). These data are consistent with previous observations that acetylated PAMAM dendrimers prevent nonselective interaction between dendrimers and cell membrane (*3*, *18*).

Cell transfection (internalization) is a complicated process. It has previously been reported that dendrimer-mediated transfection occurs mainly through active uptake (e.g. in the case of dendrimer/DNA complexes or noncharged dendrimers with a cell surface targeting moiety) (*11*). Evidence of membrane disruption caused by positively charged dendrimers has been demonstrated using model membranes such as anionic vesicles (*8*) as well as synthetic membranes with a preference for nonlamellar phases (*10*). The experimental data in this paper suggests an alternative mechanism involving the formation of 15−40 nm holes in the membrane. This proposal is consistent with the previous experiments showing dendrimer-mediated transfection and dendrimer-induced membrane disruption as well as the cytosolic enzyme leakage assays, dye diffusion, fluorescence microscopy, and AFM experiments discussed in this paper. Additional experiments are planned to fully address this question and will be the subject of future reports.

Conclusions: Relationship of These Experiments to Targeted Drug Delivery. Intracellular drug delivery has advantages over simple diffusion of drug into cells. A number of candidates for drug delivery vehicles have been evaluated mostly based on charged polymeric materials (*5*, *28*). Higher drug efficiency can be achieved with therapeutic transport agents targeted to specific cells. From our results, the positively charged polymeric material causes the formation of holes or the dendroporation of the cell membrane leading to nonselective internalization into cells. Moreover, the polycation eventually causes cell death if the concentration is high enough (>500 nM in this study). Charge neutral dendrimers, however, do not cause hole formation or den-

droporation and show no nonspecific binding or internalization. They can be internalized into the cell only if the dendrimer is linked to a targeting compound such as FA as previously described (*3*).

LITERATURE CITED

(1) Bielinska, A., Kukowska-Latallo, J. F., Johnson, J., Tomalia, D. A., and Baker, J. R. (1996) Regulation of in vitro gene expression using antisense oligonucleotides or antisense expression plasmids transfected using starburst PAMAM dendrimers. *Nucleic Acids Res. 24*, 2176−2182.

(2) Kukowska-Latallo, J. F., Raczka, E., Quintana, A., Chen, C. L., Rymaszewski, M., and Baker, J. R. (2000) Intravascular and endobronchial DNA delivery to murine lung tissue using a novel, nonviral vector. *Hum. Gene Ther. 11*, 1385−1395.

(3) Quintana, A., Raczka, E., Piehler, L., Lee, I., Myc, A., Majoros, I., Patri, A. K., Thomas, T., Mulé, J., and Baker, J. R. (2002) Design and function of a dendrimer-based therapeutic nanodevice targeted to tumor cells through the folate receptor. *Pharm. Res. 19*, 1310−1316.

(4) Esfand, R., and Tomalia, D. A. (2001) Poly(amidoamine) (PAMAM) dendrimers: from biomimicry to drug delivery and biomedical applications. *Drug Discovery Today 6*, 427−436.

(5) Gillies, E. R., and Fréchet, J. M. J. (2002) Designing macromolecules for therapeutic applications: Polyester dendrimer-poly(ethylene oxide) "bow-tie" hybrids with tunable molecular weight and architecture. *J. Am. Chem. Soc. 124*, 14137−14146.

(6) Morgan, J. R., and Cloninger, M. J. (2002) Heterogeneously functionalized dendrimers. *Curr. Opin. Drug Discovery Dev. 5*, 966−973.

(7) Langer, R. (1998) Drug delivery and targeting. *Nature 392*, 5−10.

(8) Zhang, Z. Y., and Smith, B. D. (2000) High-generation polycationic dendrimers are unusually effective at disrupting anionic vesicles: Membrane bending model. *Bioconjugate Chem. 11*, 805−814.

(9) Ottaviani, M. F., Matteini, P., Brustolon, M., Turro, N. J., Jockusch, S., and Tomalia, D. A. (1998) Characterization of starburst dendrimers and vesicle solutions and their interactions by CW- and pulsed-EPR, TEM, and dynamic light scattering. *J. Phys. Chem. B 102*, 6029−6039.

(10) Karoonuthaisiri, N., Titiyevskiy, K., and Thomas, J. L. (2003) Destabilization of fatty acid-containing liposomes by polyamidoamine dendrimers. *Colloid Surface B 27*, 365−375.

(11) Rolland, A. P. (1998) From genes to gene medicines: Recent advances in nonviral gene delivery. *Crit. Rev. Ther. Drug 15*, 143−198.

(12) Tang, M., Redemann, C. T., and Szoka, F. C. (1995) Biophysical and Chemical Determinants of Efficient Gene Delivery By Polyamidoamine Dendrimers. *J. Cell. Biochem.* 400−400.

(13) Fischer, R., Köhler, K., Fotin-Mleczek, M., and Brock, R. (2004) A stepwise dissection of the intracellular fate of cationic cell-penetrating peptides. *J. Biol. Chem. 279*, 12625−12635.

(14) Thorén, P. E. G., Persson, D., Esbjörner, E. K., Goksor, M., Lincoln, P., and Nordén, B. (2004) Membrane binding and translocation of cell-penetrating peptides. *Biochemistry 43*, 3471−3489.

(15) Mecke, A., Uppuluri, S., Sassanella, T. M., Lee, D.-K., Ramamoorthy, A., Baker, J. R., Orr, B. G., and Banaszak Holl, M. M. (2004) Direct Observation of Lipid Bilayer Disruption by Polyamidoamine Dendrimers. *Chem. Phys. Lipids*, accepted.

(16) Mecke, A., Lee, I., Orr, B. G., Banaszak Holl, M. M., and Baker, J. R. (2004) Deformability of Poly(amidoamine) Dendrimers. *Eur. Phys. J. E 14* (1), 7−16.

(17) van Duijvenbode, R. C., Borkovec, M., and Koper, G. J. M. (1998) Acid−base properties of poly(propylene imine) dendrimers. *Polymer 39*, 2657−2664.

(18) Majoros, I. J., Keszler, B., Woehler, S., Bull, T., and Baker, J. R. (2003) Acetylation of poly(amidoamine) dendrimers. *Macromolecules 36*, 5526−5529.

(19) Wiener, E. C., Konda, S., Shadron, A., Brechbiel, M., and Gansow, O. (1997) Targeting dendrimer-chelates to tumors and tumor cells expressing the high-affinity folate receptor. *Invest. Radiol. 32*, 748−754.

(20) Bielinska, A. U., Kukowska Latallo, J. F., and Baker, J. R. (1997) The interaction of plasmid DNA with polyamidoamine dendrimers: mechanism of complex formation and analysis of alterations induced in nuclease sensitivity and transcriptional activity of the complexed DNA. *BBA-Gene Struct. Expr. 1353*, 180−190.

(21) Hong, S., Bielinska, A. U., Banaszak Holl, M. M., Orr, B. G., and Baker, J. R. (2003). Unpublished work.

(22) Umebayashi, Y., Miyamoto, Y., Wakita, M., Kobayashi, A., and Nishisaka, T. (2003) Elevation of plasma membrane permeability on laser irradiation of extracellular latex particles. *J. Biochem. 134*, 219−224.

(23) Myc, A., Kukowska-Latallo, J. F., Bielinska, A. U., Cao, P., Myc, P. P., Janczak, K., Sturm, T. R., Grabinski, M. S., Landers, J. J., Young, K. S., Chang, J., Hamouda, T., Olszewski, M. A., and Baker, J. R. (2003) Development of immune response that protects mice from viral pneumonitis after a single intranasal immunization with influenza A virus and nanoemulsion. *Vaccine 21*, 3801−3814.

(24) Myc, A., Arscott, P. L., Bretz, J. D., Thompson, N. W., and Baker, J. R. (1999) Characterization of FAP-1 expression and function in thyroid follicular cells. *Endocrinology 140*, 5431−5434.

(25) Jevprasesphant, R., Penny, J., Jalal, R., Attwood, D., McKeown, N. B., and D'Emanuele, A. (2003) The influence of surface modification on the cytotoxicity of PAMAM dendrimers. *Int. J. Pharm. 252*, 263−266.

(26) Andersson, M. M., Hatti-Kaul, R., and Brown, W. (2000) Dynamic and static light scattering and fluorescence studies of the interactions between lactate dehydrogenase and poly-(ethyleneimine). *J. Phys. Chem. B 104*, 3660−3667.

(27) Baldwin, T. O., Christopher, J. A., Raushel, F. M., Sinclair, J. F., Ziegler, M. M., Fisher, A. J., and Rayment, I. (1995) Structure of bacterial luciferase. *Curr. Opin. Struct. Biol. 5*, 798−809.

(28) Fischer, D., Li, Y. X., Ahlemeyer, B., Krieglstein, J., and Kissel, T. (2003) In vitro cytotoxicity testing of polycations: influence of polymer structure on cell viability and hemolysis. *Biomaterials 24*, 1121−1131.